

# Zincating morphology of aluminum bond pad: its influence on quality of electroless nickel bumping

Guojun Qi<sup>a,\*</sup>, Lambertus G.J. Fokkink<sup>a</sup>, Kee Heng Chew<sup>b</sup>

<sup>a</sup>*Gintic Institute of Manufacturing Technology, 71 Nanyang Drive, Singapore 638075, Singapore*

<sup>b</sup>*Queensland University of Technology, Queensland, Australia*

Received 22 June 2001; received in revised form 23 October 2001; accepted 30 November 2001

## Abstract

This work relates to the electroless nickel (EN) metallization and bumping processes for flip chip packaging applications. Zincating of the aluminum bond pads is an essential process step, activating the pads for EN deposition and ensuring good adhesion between the pad and the bump. Different zinc layer morphologies in terms of grain size or smoothness are reproducibly prepared by varying the zincating process parameters and chemical conditions. Quantitative correlations between the zinc layer morphology and the bump characteristics have been established. © 2002 Elsevier Science B.V. All rights reserved.

**Keywords:** Electroless nickel; Wafer bumping; Aluminum, Zincate

## 1. Introduction

The relentless miniaturization drive, together with the demand for higher performance and functionality of portable electronics products, such as notebook PCs and hand phones, translates into the use of smaller electronic packages with higher I/O counts operating at higher frequencies. Forecasts [1,2] show that high-performance packages (BGA, CSP, DCA, etc.) will account for approximately 50% of annual market share growth in the coming years, which could represent up to one third of the multi-billion dollar market.

Flip chip packaging technology is currently the most promising approach to satisfy the high-end packaging market. A key contributor to this technology is wafer bumping, whereby interconnection metallic bumps are built on the chip's I/O pads. When the chip is 'flipped over' and attached to a matching pattern on a substrate, the bumps provide the interconnection, which is conventionally achieved by wire bonding. Among the various bumping methodologies, the electroless nickel (EN) metallization and bumping process is relatively low cost

and straightforward [3–11]. In cases where multi-element lead-free solder is difficult to deposit by electroplating, electroless nickel metallization plus other direct solder application techniques, such as stencil printing, will be a more feasible processing route.

Aluminum, with minor doping of other elements, is the dominant material for IC bond pad metallization. This will remain true for some time, even taking into consideration the newly emerging copper metallization schemes. Aluminum is catalytic for electroless nickel deposition. However, as aluminum instantaneously oxidizes during rinsing or exposure to air, the oxide films will completely suppress metallization or prevent the formation of intermetallic bonds between the EN and substrate, resulting in adhesion failure. Zincating of the aluminum pads is a widely used process step that activates the pads for subsequent EN deposition, which, in principle, gives rise to good adhesion between pad and bump. Zincating relies on the electrochemical exchange reaction between zinc complexes in solution and aluminum metal, depositing zinc crystallites at the expense of aluminum dissolution (etching). Although there have been studies [12,13] on various aspects of zincating treatment of bulk aluminum alloys, systematic work on its influence on bump performance is lacking and there is no clear understanding yet as to how the

\*Corresponding author. Tel.: +65-793-8383; fax: +65-791-6377.  
E-mail address: gjq@gintic.gov.sg (G. Qi).

zincating layer morphology affects the bumps with respect to adhesion, electrical reliability, etc. The aim of this work is to gain qualitative and quantitative insights into the relationships between the zincating operation and the adhesion of the final EN bumps.

Different zinc layer morphologies, in terms of grain size, smoothness and coverage, are obtained by varying the process parameters. Quantitative correlations between the morphology obtained and process parameters have been established. Correlations are presented between the zincating morphology and bump quality measurements, such as bump morphology and shear strengths.

## 2. Experimental

The test vehicles used in this study were prepared from blank wafers. A pure aluminum film ( $\sim 1 \mu\text{m}$  thickness) was deposited onto the polished side of the wafers with an unbalanced magnetron sputtering system. Standard photolithography and wet etching procedures were used to produce  $50 \times 50 \mu\text{m}$  square and  $100 \mu\text{m}$  diameter round pads in both peripheral and area array patterns. The test wafers were then diced into smaller segments for the experiments. Different pad geometry and arrangements were adopted to check their possible influence to zincating quality. The sputtered aluminum film's mirror finish did not change after the photolithography and etch processing. A commercial alkaline-based zincating solution concentrate from Enthone-OMI was used as the base solution for the zincating experiment. Dilution of the concentrate was done using 1 M NaOH. An in-house developed electroless Ni-P solution, based on  $\text{NiSO}_4$  as the metal source and hypophosphite as the reducing agent, was used for EN plating.

Initial experiments showed the zinc layer morphology to vary with zincating process parameters (temperature, immersion time, number of immersion repetitions, etc.) and zincating chemistry. It was found later that different but reproducible zincating morphologies could be obtained using various diluted solutions of the OMI concentrate solution. All zincating and EN bumping samples reported here were prepared by using part or all of the following process steps, varying the zincating solution only:

1. mild etching/cleaning with weak alkaline cleaner (ENBOND<sup>®</sup>-5979, OMI), 70–75 °C, 60 s;
2. rinsing with deionized (DI) water, room temperature (RT);
3. first zincating; 45 s, RT;
4. rinsing with DI water, RT;
5. nitric acid dip; 20%  $\text{HNO}_3$ , 15 s, RT;
6. rinsing with DI water, RT;
7. second zincating; 15 s, RT;
8. rinsing with DI water, RT;

9. electroless nickel bumping, 88 °C, 10 to 60 min; and
10. rinsing with DI water.

Samples were taken at various stages of the process, steps (4, 6 and 9) and analyzed by several techniques. Scanning Electron Microscopy (SEM) observation provided visual comparison. Image analysis was performed on the SEM images to quantify the grain sizes and coverage of the pad by zinc crystals. A stylus profilometer (Talysurf Series 2, Talyor-Hobson) was used to measure the roughness of the zinc layer. Shear strength of the EN bumps was used to characterize adhesion of the bumps to the aluminum pads. It was measured with a Dage-4000 shear/pull tester with a constant machine setting. In the shear test, the load continuously increases after the shear tool comes in contact with a bump, until the bump is pushed off from the pad. The force required to displace the bump is identified as the shear force of the bump. Shear strength data are expressed as shear force per unit pad area.

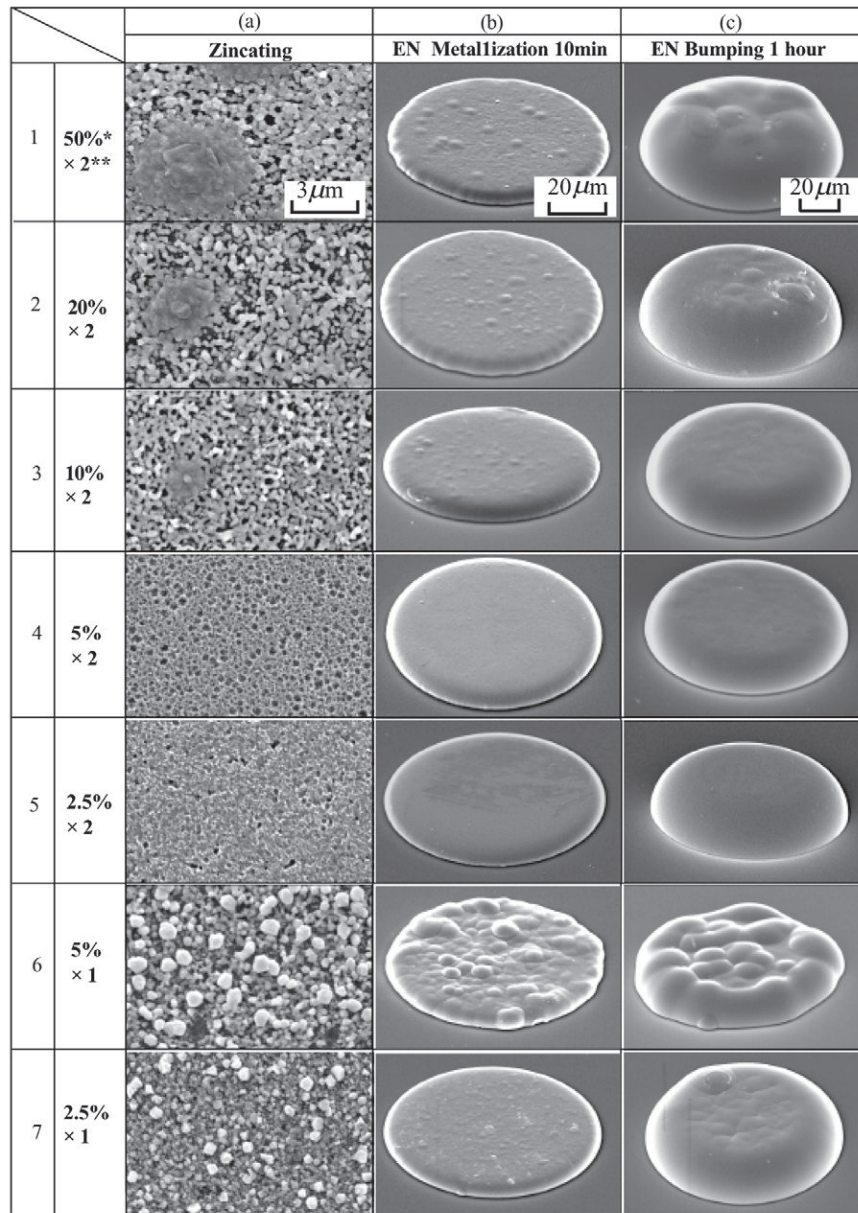
## 3. Results and discussion

### 3.1. Zincating morphology

Representative electromicrographs of the zincated samples treated with different dilutions of the standard OMI concentrate are shown in the first column of Fig. 1, (1–7a). Among them, the first five photos (1–5a) are from samples obtained by double zincating (steps 1–8 described in Section 2) and the remainder (6–7a) by single zincating (steps 1–4). The 50%-diluted solution is that recommended by the supplier for treating bulk aluminum parts. Very little zinc coverage of the pads was observed in the case of single zincating with 20% and 50% diluted solutions, and those samples were excluded from this study. It was noticed that the bump size and their pattern had no effect on the resultant zincate morphologies.

It is observed that double zincating gives significantly smaller crystals and more uniform coverage of the aluminum surface compared with a single zincating treatment. During the experiment, we noticed that the nitric acid etching removed most, if not all, of the zinc deposited in the first zincating treatment. No zinc signal could be detected from the etched samples by Energy Dispersive X-ray (EDX) analysis, even at very low electron acceleration voltages, although the 'foot prints' of the zinc crystallites were visible from SEM images. The mechanism is, however, not clear as how the acid etching helps to achieve the smoother zinc deposition in the second zincating treatment.

From the SEM images shown in Fig. 1, it is evident that the morphology of the zinc crystals varies signifi-



\* Dilution of the base solution (percentage of the concentrate in the final solution)

\*\* Number of zincating treatments, either single or double

Fig. 1. Variation of zinc and EN deposition morphologies with zincating chemistry.

cantly with solution concentration. Very regular and smooth zinc layers are obtained for the lowest concentrations of zincating solution. Nodular agglomerates of zinc crystallites are present when high concentrations are used. They are observed in increasing size and numbers for 10%, 20% and 50% dilutions.

As a quantitative description of the zinc layer morphology, the average diameters,  $\phi_{av}$ , of the individual zinc crystals was obtained from image analysis. In addition, as a measure of the size of the crystallites, the surface roughness, Ra and Rp, of zincated pads were measured with the profilometer. Ra is the arithmetic

mean of the departure of the profile from the average height and Rp the maximum height of the profile above the average level. A very clear correlation between  $\phi_{av}$ , Ra, and Rp is observed in Fig. 2, suggesting that all three parameters give a reliable indication of crystallite size. More importantly, it is seen that a distinct influence of the solution concentration on the crystallite size exists: further-diluted solutions give finer zinc crystals. Our measurements clearly demonstrate that zinc coverage of the aluminum pads is significantly affected by the process conditions, including the concentration, of the zincating solution.

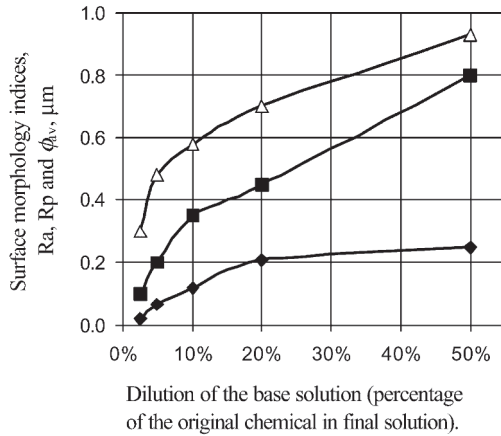


Fig. 2. Correlation of surface morphology indices with zincating chemistry.

### 3.2. Influence of zincating on EN metallization and bumping

EN metallization refers to the deposition of a thin layer of electroless nickel, usually 3–5 μm in thickness, as an under bump metallurgy (UBM) for bumping of ICs/wafers with other materials like eutectic Sn–Pb solder, while EN bumping aims to grow the EN to such a thickness as to form a complete bump (~20 μm). The morphologies of EN metallization and bumping initiated from differently zincated pads, as discussed above, are also shown in Fig. 1, columns b and c, respectively. As we selected a carefully optimized experimental electroless solution, that is known to deposit very smooth bumps on evenly-activated structures (see, e.g. Fig. 1, c5), the effects of zincating morphologies on the appearance of UBMs and bumps can be directly derived from the electronmicrographs. The roughness of the zinc layer will inevitably be transferred to the EN, especially for the thin metallization, where the leveling effect of EN plating does not have enough time to ‘smooth’ the surface. If granted longer plating time, the minor unevenness of the zinc layer may be leveled out. This is true only for continuous and even zinc coverage. Under conditions where the zincating process results in the formation of large zinc agglomerates on the pads, distinct protrusions in the EN (even for the 20-μm thick deposits!) are observed (Fig. 1, c1, c2, c6 and c7). This might be detrimental to the subsequent flip chip assembly process.

### 3.3. Correlation of zincating morphology and bump shear strength

As evidenced by our shear strength measurements, a distinct influence of the zincating treatment on the bump adhesion exists. The adhesion of the EN bumps represented by the shear strength varies with the zinc mor-

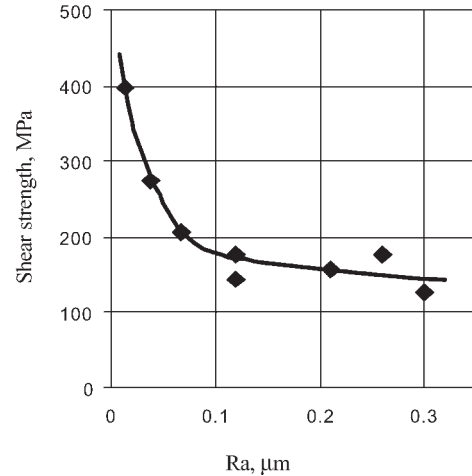


Fig. 3. Correlation of bump shear strength with the surface roughness on the zinc layer, Ra.

phology. Fig. 3 shows the correlation of the shear strength with Ra. The general trend is that the smoother and more fine-grained the zinc layer, the higher the strength, though the change becomes very pronounced when  $Ra < 0.1 \mu\text{m}$ , leading to a distinct ‘kink’ in the shear strength behavior at approximately 200 MPa.

Representative failure modes of the bumps before and after the kink in Fig. 3 are compared in Fig. 4. For bumps grown on a zinc layer with  $Ra < 0.1 \mu\text{m}$ , cohesive failure of aluminum was observed as shown in Fig. 4a, while for bumps on coarser zinc layers failure occurs in the interface of aluminum and EN, as shown in Fig. 4b.

It is interesting to note that the round nodules (as indicated by the arrow in Fig. 4b) were of similar appearance to the zinc agglomerates seen in Fig. 1, 1–3a. EDX analysis revealed that iron (present as an

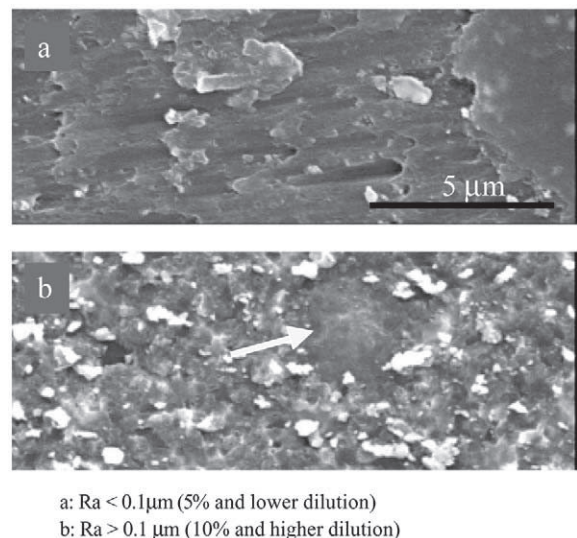


Fig. 4. Comparison of failure modes in bump shear test.

additive in the zincating concentrate) is present in both structures. This suggests that the zinc crystal agglomerates resulting from poor zincating form weak points in the EN to aluminum joint.

Good adhesion of the bump materials to the aluminum pad is required to maintain the mechanical integrity and electrical functionality of the IC after packaging. For a UBM plus solder bump structure, the general requirement for adhesion is that the bump should fail within the solder, when subjected to stress. This means that the adhesion strength of the UBM to aluminum and to the solder should be higher than the cohesive strength of the solder. For eutectic tin-lead solder the cohesive strength is approximately 30–60 MPa (3–6 kg/mm<sup>2</sup>), which is lower than any of the shear strength values shown in Fig. 3. This implies that as a metallization or UBM for solder bumping, the EN depositions obtained by all the zincating treatments discussed above are mechanically acceptable from the adhesion point of view.

Compared with the shear strength of gold bumps in flip chip on glass (FOG) applications (60–170 MPa, depending on annealing conditions), and considering that EN is harder and stronger than gold, an acceptable shear strength for EN bumps should be higher than that of gold. Therefore, a minimum value of 200 MPa seems reasonable. To meet this requirement, good zincating treatment of the pads, leading to zinc layer roughness (Ra) of approximately 0.1 μm, is an absolutely necessity. This also leads to very smooth EN deposits, both as UBM and as full bumps. The morphologies and failure modes shown in Fig. 1 (4a and 5a) and Fig. 4a, therefore, provide a meaningful benchmark.

#### 4. Concluding remarks

Different zinc layer morphologies in terms of grain size or smoothness were studied. Quantitative correlations between the zinc layer morphology and process parameters have been established. More diluted zincating solutions from the OMI concentrate lead to smooth and small-grained zinc layers. Correlations are presented between the zincating morphology and bump quality measurements, such as morphology of the bump and

shear strength. The general trend is that the smoother and more fine-grained the zinc layer, the higher the shear strength.

Results discussed here have important technical implications. Proper zincating of aluminum pads is an absolute requirement for the production of smooth and well-adherent bumps. The zincating treatment has to be carefully examined and the resultant zincating morphology under control before a reliable EN bumping process can be launched. In addition, in combination with the zincating process, an optimized electroless nickel solution is mandatory for the production of reliable and morphologically sound bumps. EN solutions that work well for bulk aluminum plating, often do not produce acceptable results for wafer bumping (rough bumps, missing bumps, etc.). Our results may serve as a reference for the development of reliable industrial-scale EN metallization and bumping processes, although specific effects concerning such factors as pad material and behavior of the EN solution must be assessed on a case-by-case basis.

#### References

- [1] S. Berry, *High-Density Interconnect 1* (1998) 14.
- [2] J. Murry, *High Density Interconnect 1* (1998) 40.
- [3] K. Wong, K. Chi, A. Rangappan, *Plat. Surf. Finish.*, July (1988) 70.
- [4] J. Simon, E. Zakel, H. Reichl, *Met. Finish.*, Oct. (1990) 23.
- [5] A. Aintila, E. Jarvinen, S. Lalu, *Proceedings of IEMT, Kanazawa, Japan, 1993*, p. 33.
- [6] J. Liu, *Hybrid Circuits* 29 (1992) 25.
- [7] E. Queau, G. Streamsdoerfer, J.R. Martin, P. Clechet, *Plat. Surf. Finish.*, Jan. (1994) 67.
- [8] A. Aintila, A. Bjorklof, E. Jarvinen, S. Lalu, *Proceedings of the 1994 IEEE/CPMT International Electronics Manufacturing Technology Symposium, 1994*, p. 160.
- [9] A. Bjorklof, *Microelectron. Int.* 40 (1996) 49.
- [10] T. Ohtsuka, T. Kawakita, H. Fujimoto, K. Hatada, *Proceedings of the Joint International Electronic Manufacturing Symp. and International Microelectronics Conference, 1997*, p. 169.
- [11] J. Kloeser, A. Ostmann, J. Gwiasda, F. Bechtold, R. Aschenbrenner, H. Reichl, *Int. J. Microcircuits Electron. Packag.* 20 (1997) 383.
- [12] F.J. Monteiro, M. Barbosa, D.R. Gabe, D.H. Ross, *Surf. Coat. Technol.* 35 (1988) 321.
- [13] F.J. Monteiro, M. Barbosa, D.R. Gabe, D.H. Ross, *Met. Finish.*, Oct. (1989) 49.